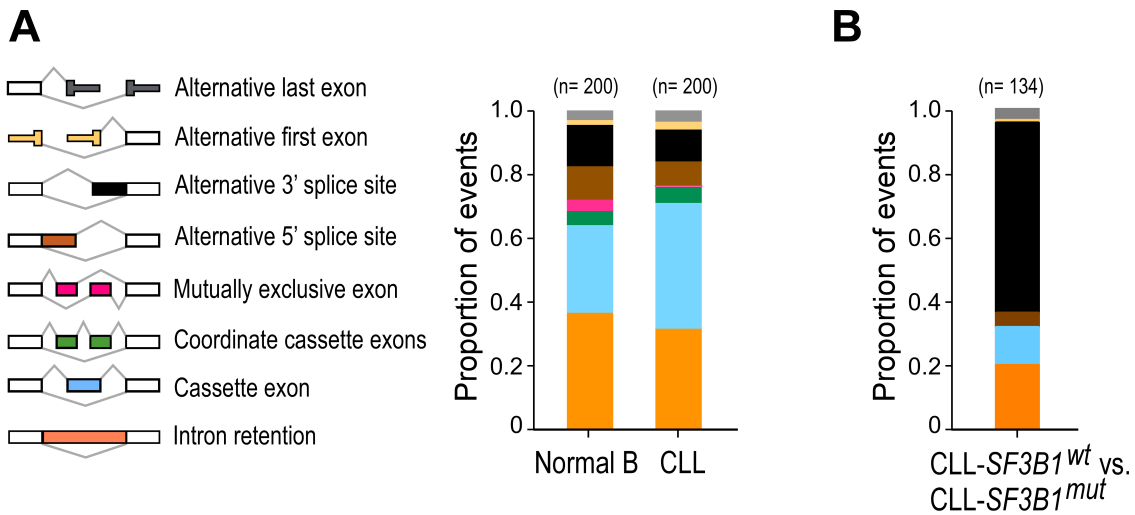


SUPPLEMENTAL MATERIAL

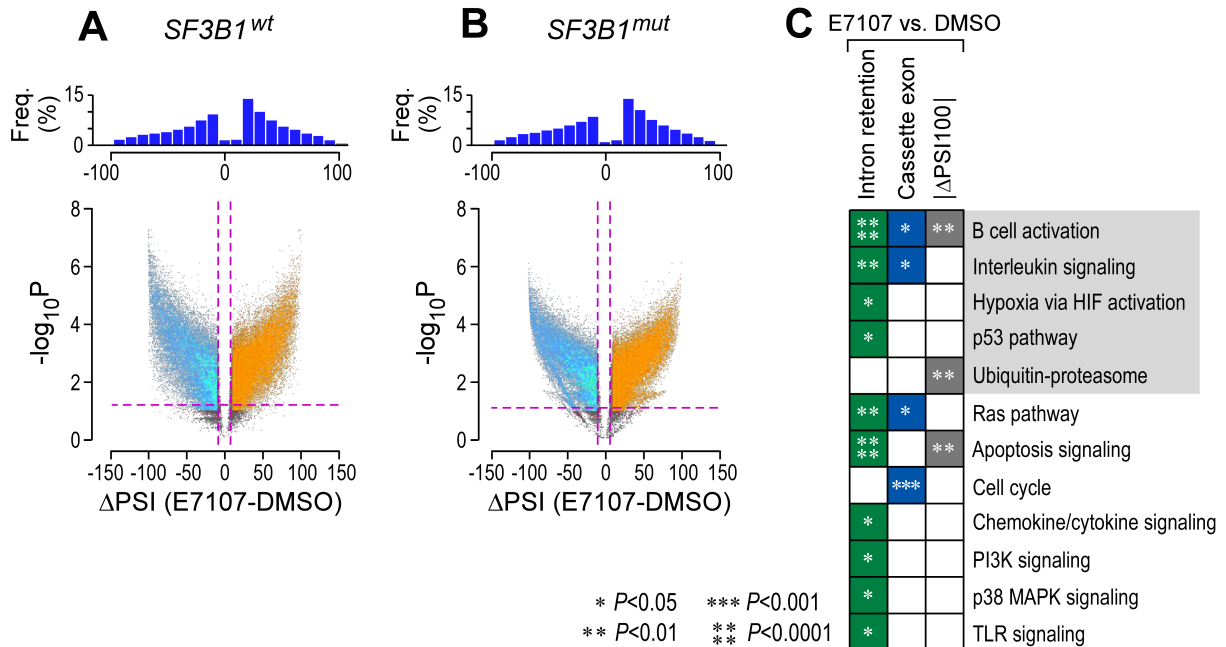
Splicing modulation sensitizes chronic lymphocytic leukemia cells to venetoclax by remodeling mitochondrial apoptotic dependencies

Elisa ten Hacken, Rebecca Valentin, Fara Faye D. Regis, Jing Sun, Shanye Yin, Lillian Werner, Jing Deng, Michaela Gruber, Jessica Wong, Mei Zheng, Amy L. Gill, Michael Seiler, Peter Smith, Michael Thomas, Silvia Buonamici, Emanuela M. Ghia, Ekaterina Kim, Laura Z. Rassenti, Jan A. Burger, Thomas J. Kipps, Matthew L. Meyerson, Pavan Bachireddy, Lili Wang, Robin Reed, Donna Neuberg, Ruben D. Carrasco, Angela N. Brooks, Anthony Letai, Matthew S. Davids, Catherine J. Wu

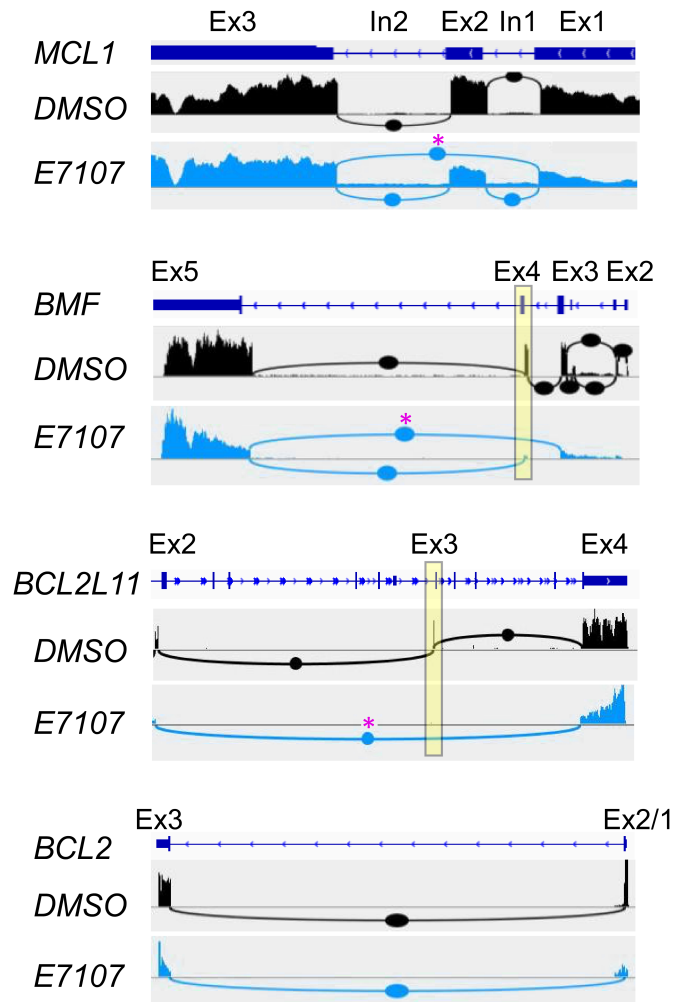
SUPPLEMENTAL FIGURES



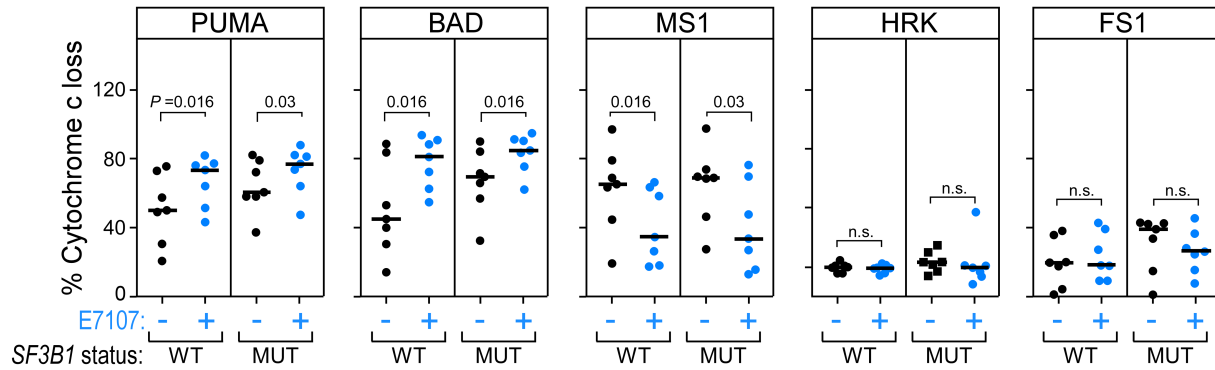
Supplemental Figure 1. Alternative splicing patterns in normal B cells and CLL. (A) Proportion of events within splicing categories of the 200 most variable splice events based on analysis of RNA-seq data from 7 normal B cell samples and 22 CLL samples. **(B)** Proportion of events within splicing categories of the 134 differential splice events based on analysis of RNA-seq data from 13 CLL-*SF3B1*^{wt} compared to 9 CLL-*SF3B1*^{mut} samples.



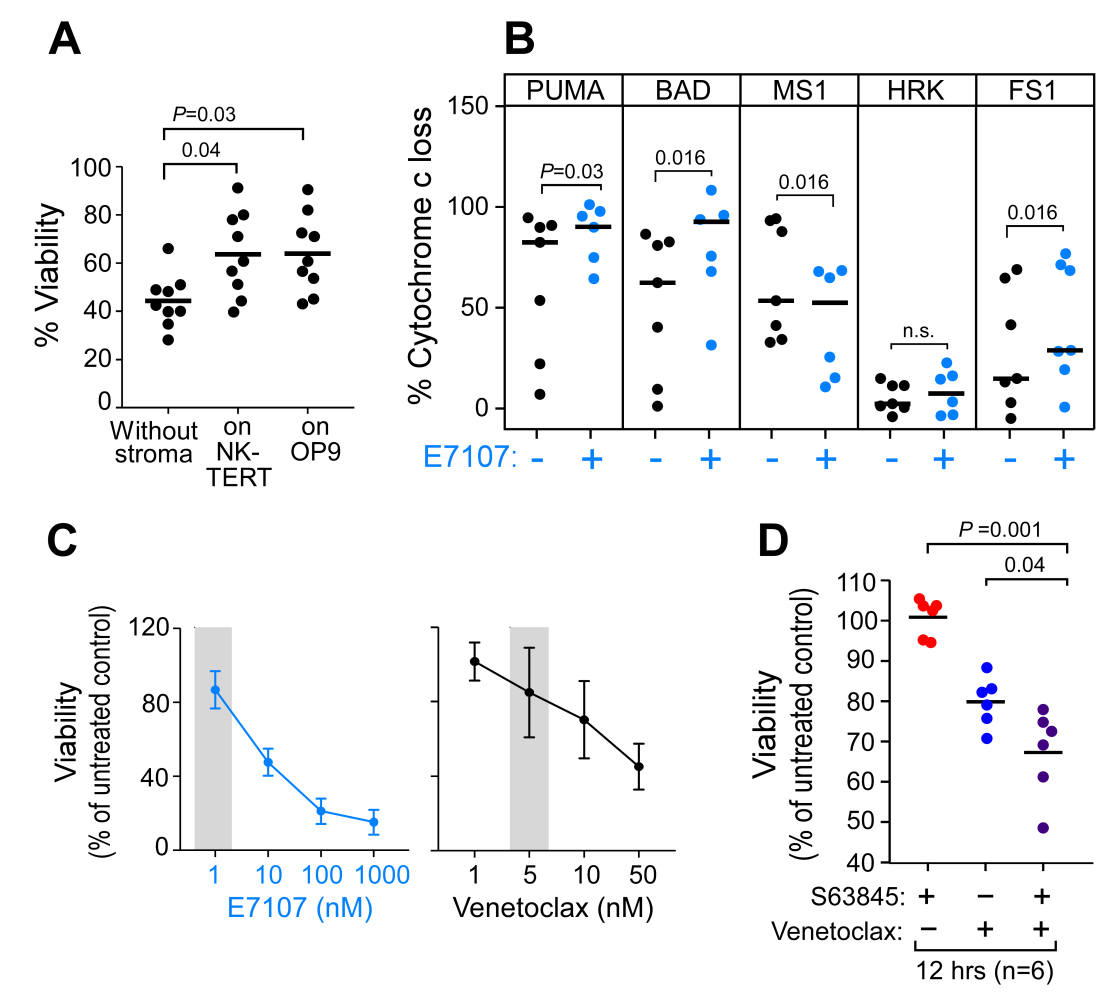
Supplemental Figure 2. Splicing modulation broadly affects the CLL transcriptome, irrespective of *SF3B1* mutation status. Frequency of delta Percent Spliced In (Δ PSI) for significant splice changes from the RNA-Seq data of (A) 6 *SF3B1*^{wt} and (B) 5 *SF3B1*^{mut} after 8 hours of treatment with 5nM E7107 compared to DMSO treated controls and volcano plot of Δ PSI versus negative logarithmic P values ($-\log_{10}P$) of all splicing changes. Pink dashed lines: thresholds of $|\Delta$ PSI| of 10% and FDR of 10% (i.e. $-\log_{10}P=1$) for significant splice changes. Orange dots: intron retention events; light blue dots: cassette exon events; grey dots: all other categories of splice events. (C) Pathway enrichment analysis by Panther algorithm of the 1000 most significant intron retention and the 1000 most significant cassette exon events, and the 471 events with $|\Delta$ PSI|=100 within the significantly modulated events after E7107 treatment as compared to DMSO control. The grey shaded area highlights pathways also enriched in **Figure 1E**. Significant P values are indicated in the Figure.



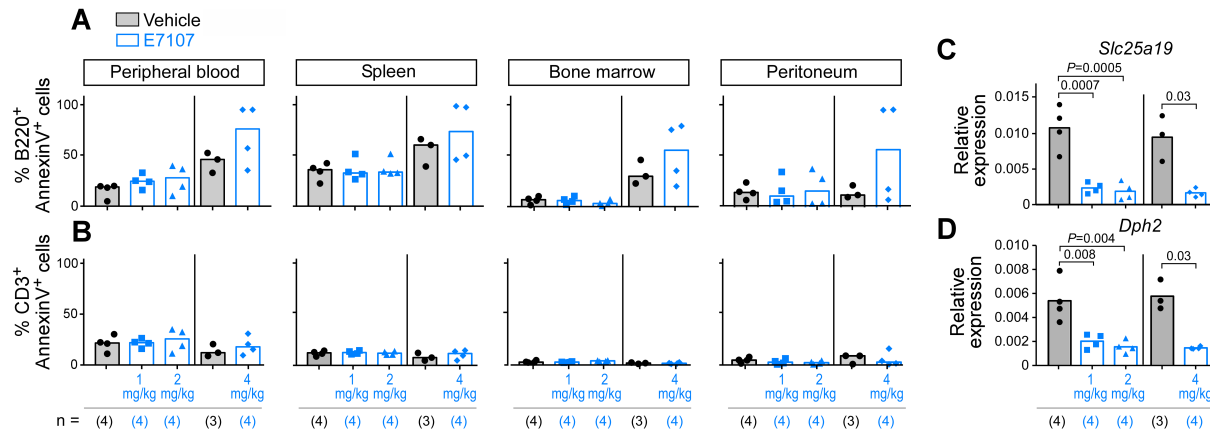
Supplemental Figure 3. Splicing modulation by E7107 differentially affects splicing junctions in BCL2 family members. Representative Sashimi plots of the *MCL1*, *BMF*, *BCL2L11* and *BCL2* genes showing splicing junctions after treatment with DMSO or E7107. Novel splicing junctions introduced by E7107 treatment are marked with a pink “*”.



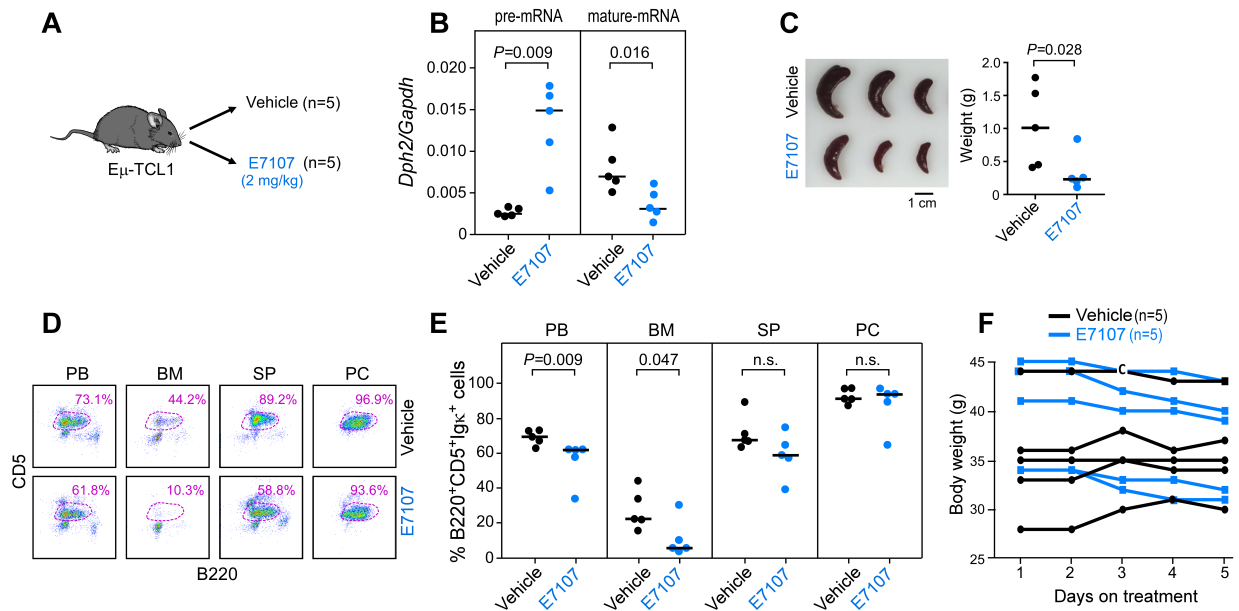
Supplemental Figure 4. BH3 profiling analysis shows concordant modulation of signals across CLL samples after E7107 treatment. Percentage (%) Cytochrome c loss as quantified by flow cytometry before and after overnight treatment of 14 CLLs subdivided based on *SF3B1* mutation status (7 *SF3B1*^{wt}, 7 *SF3B1*^{mut}) with 3nM E7107 in the presence of NK-TERT stroma. Panels from left to right refer to PUMA (overall priming), BAD peptide (BCL2 dependence), MS1 (MCL1 dependence), HRK (BCLxL dependence), FS1 (BFL1 dependence). Reported *P* values were calculated by Wilcoxon signed-rank test.



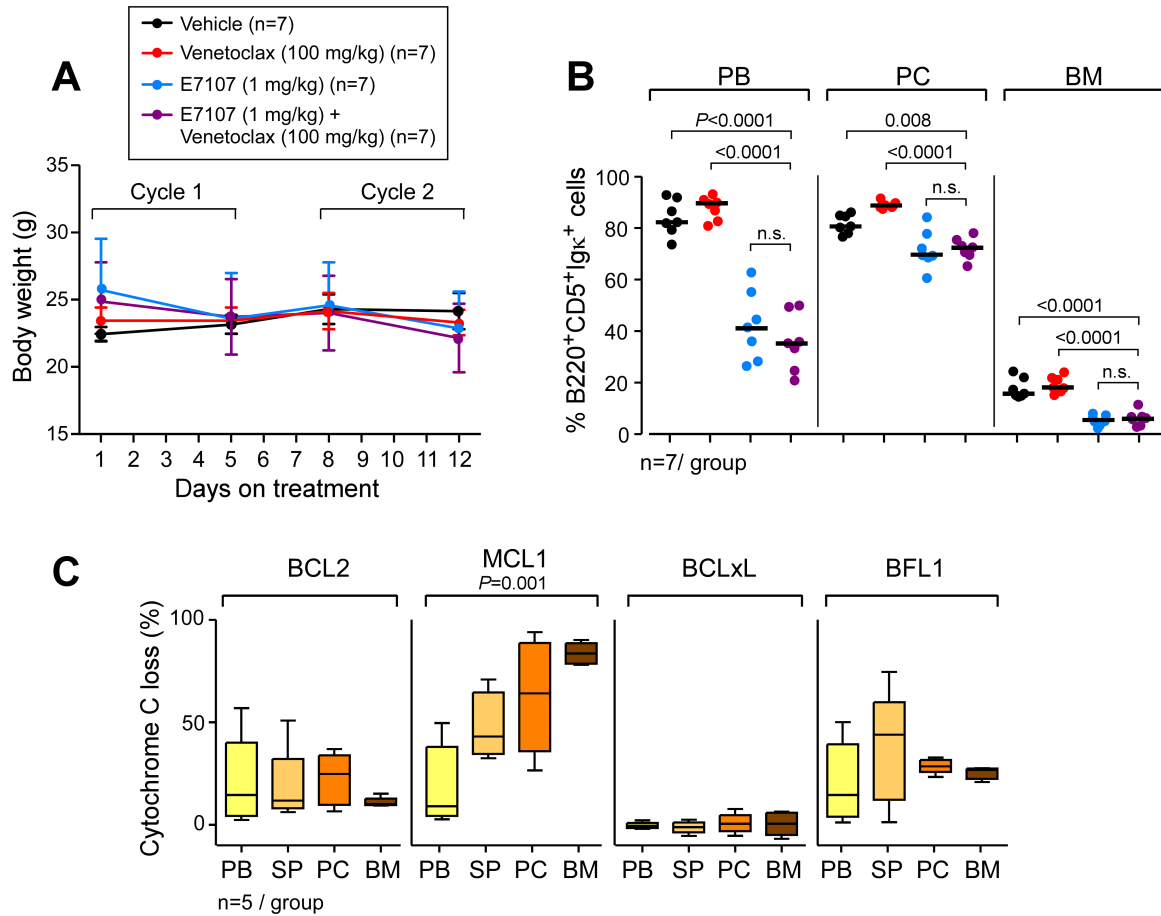
Supplemental Figure 5. Establishment of experimental conditions for *in vitro* assays on human and murine CLL cells, and BH3 profiling of E μ -TCL1 splenocytes after E7107 treatment. (A) Percentage (%) viability of 9 CLLs upon overnight incubation in the absence of stromal support or on either NK-TERT or OP9 stroma. *P* values were calculated by ANOVA with Scheffé's correction for multiple comparisons. (B) Percentage (%) Cytochrome c loss as quantified by flow cytometry on 7 TCL1 splenocyte preparations before and after 4 hours of treatment with 5nM E7107 on OP9 stroma. Panels from left to right refer to PUMA (overall priming), BAD peptide (BCL2 dependence), MS1 (MCL1 dependence), HRK (BCLxL dependence), FS1 (BFL1 dependence). Reported *P* values were calculated by Wilcoxon signed-rank test. (C) Mean \pm SD of percentage (%) viability of 4 TCL1 splenocyte preparations treated with increasing concentration of E7107 (left panel), or with increasing concentrations of venetoclax (right panel), overnight on OP9 stroma. Grey shaded areas indicate the drug concentrations chosen for the combination studies displayed in **Figure 5D. (D) Percent (%) viability of the untreated control of 6 TCL1 samples after overnight treatment with 1nM S63845, 5nM venetoclax or their combination, on OP9 stroma. Reported *P* values were calculated by one-way ANOVA with Scheffé's correction for multiple comparisons.**



Supplemental Figure 6. Dose range finding studies of E7107 in C57BL/6 wild type animals. (A) Percentage (%) apoptotic normal B cells (B220⁺AnnexinV⁺) and (B) T cells (CD3⁺ AnnexinV⁺) in the peripheral blood, spleen, bone marrow and peritoneum of mice treated with either vehicle control (black) or increasing concentrations (1-4mg/kg) E7107 (light blue) for 4 days. Vertical lines demarcate independent experiments. The number of animals/group are indicated in brackets below the corresponding bar. (C) Relative expression of mature RNA levels of *Slc25a19* (normalized to *Gapdh*) following 3 hours of treatment with 1-4mg/kg E7107 or vehicle control. *P* values were calculated by ANOVA with Scheffé's correction for multiple comparisons for the first three groups, by Mann Whitney *U* test for the remainder two. (D) Relative expression of mature RNA levels of *Dph2* (normalized to *Gapdh*) following 3 hours of treatment with 1-4mg/kg E7107 or vehicle control. *P* values were calculated by one-way ANOVA with Scheffé's correction for multiple comparisons for the first three groups, by Mann Whitney *U* test for the remainder two.



Supplemental Figure 7. Treatment with single agent E7107 reduces leukemia burden in E μ -TCL1 mice. (A) Treatment schema of 12-month old E μ -TCL1 animals (5 animals/group) treated for a week with either vehicle control or 2mg/kg E7107. (B) Relative expression of *Dph2* pre-mRNA and mature-mRNA (normalized to *Gapdh*) in the blood of vehicle control (black) or E7107 (light blue) treated animals, as analyzed 3 hours after the first E7107 dose. *P* values were calculated by Mann Whitney *U* test. (C) Representative spleens of 3 vehicle control treated and 3 E7107 treated animals, as harvested at the end of treatment. Spleen weights are expressed in grams (g), and a 1cm scale bar is indicated in the figure (n=5/group). *P* values were calculated by Mann Whitney *U* test. (D) Representative flow cytometry analyses of B220⁺CD5⁺ CLL cells in the peripheral blood (PB), bone marrow (BM), spleen (SP), or peritoneum (PC) of one animal per group. (E) Percentage (%) B220⁺CD5⁺Ig κ ⁺ CLL cells in the PB, BM, SP and PC, as analyzed by flow cytometry at the end of treatment. *P* values were calculated by Mann Whitney *U* test. (F) Body weight measurements expressed in grams (g) of vehicle control and E7107 treated animals throughout the 5-day treatment period.



Supplemental Figure 8. Combination treatment studies of E7107 and venetoclax in E μ -TCL1 based transplants. (A) Body weight measurements expressed in grams (g) of CD45.1 transplanted mice belonging to the 4 treatment groups (black: vehicle control; red: 100mg/kg venetoclax; light blue: 1mg/kg E7107; purple: combination of 1mg/kg E7107 and 100mg/kg venetoclax) at the beginning and at the end of each treatment cycle. (B) Percentage (%) B220⁺CD5⁺Igκ⁺ CLL cells in the peripheral blood (PB), peritoneal cavity (PC), and bone marrow (BM) of CD45.1 transplants, as analyzed by flow cytometry at the end of treatment. Reported *P* values were calculated by one-way ANOVA with Scheffé's correction for multiple comparisons. (C) BH3 profiling analysis of CLL cells derived from the PB, spleen (SP), PC, and BM of 5 TCL1 mice. Panels from left to right refer to percentage (%) Cytochrome c loss after incubation with 1μM BAD peptide (BCL2 dependence), 1μM MS1 (MCL1 dependence), 1μM HRK (BCLxL dependence), 1μM FS1 (BFL1 dependence). Reported *P* value was calculated by two-way ANOVA.

SUPPLEMENTAL TABLES

Supplemental Table 1, related to Figures 1A-E and Supplemental Figure 1.

Patient ID number and *SF3B1* mutational status of RNA-sequenced samples re-analyzed from our previous study ¹. MUT: mutated; WT: wild-type.

Patient ID	<i>SF3B1</i> status
CLL005	WT
CLL014	WT
CLL024	WT
CLL032	MUT (K700E)
CLL035	WT
CLL037	MUT (K700E)
CLL043	MUT (K700E)
CLL047	WT
CLL048	WT
CLL059	MUT (K700E)
CLL060	MUT (R625L)
CLL061	MUT (K700E)
CLL073	WT
CLL090	WT
CLL093	WT
CLL108	WT
CLL109	MUT (K666Q)
CLL169	MUT (K700E)
CLL170	WT
CLL193	WT
CLL194	WT
CLL195	MUT (K700E)

Supplemental Table 2, related to Figure 1E.

Pathway enrichment analysis results of the 192 most differential splicing events within CLL compared to normal B cells, and the CLL-specific splicing outliers represented in at least 7 out of 22 CLL samples (n=1138). Pathways enriched within each category, *P* values, and corresponding genes are included in the table. “*” highlights the pathways displayed in **Figure 1E**.

Normal B vs. CLL differential splicing (n=192)	P-value	-Log₁₀P	Genes
T cell activation_Homo sapiens_P00053	9.123E-06	5.040	VAV3;PPP3CB;PTPRC;PPP3CC;LCK;NFATC1
*B cell activation_Homo sapiens_P00010	3.826E-05	4.417	VAV3;PPP3CB;PTPRC;PRKCB;NFATC1
PDGF signaling pathway_Homo sapiens_P00047	0.0067	2.175	ARHGAP9;VAV3;RASA4;RPS6KB2
*Notch signaling pathway_Homo sapiens_P00045	0.0264	1.578	NCSTN;RBPJ
Alzheimer disease-presenilin pathway_Homo sapiens_P00004	0.0284	1.547	NCSTN;DVL3;RBPJ
*Wnt signaling pathway_Homo sapiens_P00057	0.0383	1.416	PPP3CB;PPP3CC;PRKCB;DVL3;NFATC1

Splicing outliers enriched in CLL (n=1138)	P-value	-Log₁₀P	Genes
*De novo purine biosynthesis_Homo sapiens_P02738	0.0026	2.579	ADSL;RRM1;IMPDH2;NME3;GART;ADSS
T cell activation_Homo sapiens_P00053	0.0072	2.142	PPP3CA;NRAS;PPP3CC;HLA-DMB;AKT2;ITPR1;LCP2;CSK;SOS2;NFKB1
*Interleukin signaling pathway_Homo sapiens_P00036	0.0083	2.081	NRAS;IL4R;SHC1;IL10RA;MKNK1;MYC;AKT2;MKNK2;IL6ST;SOS2;MTOR
*Ubiquitin proteasome pathway_Homo sapiens_P00060	0.0092	2.035	SMURF2;UBA7;MDM2;WWP2;UBE2G1;UBA1;UBE2A
PDGF signaling pathway_Homo sapiens_P00047	0.0097	2.013	ARHGAP9;PDGFRA;SHC1;ITPR1;FLI1;ARHGAP4;NRAS;MYC;AKT2;MKNK1;MKNK2;PLCG2;SOS2
*B cell activation_Homo sapiens_P00010	0.0134	1.871	LYN;PPP3CA;NRAS;CD19;ITPR1;BLNK;PLCG2;SOS2
Parkinson disease_Homo sapiens_P00049	0.0146	1.835	LYN;HSPA9;FGR;PSMA5;CSNK1G3;PSMA4;ADRBK2;CUL1;CSK;NDUFV2
*Cholesterol biosynthesis_Homo sapiens_P00014	0.0205	1.688	FDPS;HMGCR;FDFT1

CCKR signaling map ST_Homo sapiens_P06959	0.0226	1.646	LYN;ROCK1;SHC1;ODC1;PXN;ITPR1;AR HGAP4;PPP3CA;MYC;CASP3;BAX;CTN NB1;PTK2B;CSK;CALM1;MEF2D
*Coenzyme A biosynthesis_Homo sapiens_P02736	0.0403	1.395	PANK2;PANK3
*Hypoxia response via HIF activation_Homo sapiens_P00030	0.0422	1.374	CREBBP;AKT2;HIF1A;MTOR
*Oxidative stress response_Homo sapiens_P00046	0.0422	1.374	MAX;MKNK1;MYC;MKNK2
*p53 pathway_Homo sapiens_P00059	0.0440	1.357	KAT2B;CREBBP;GADD45B;HDAC1;AKT 2;MDM2;BAX;MTA2

Supplemental Table 3. Clinical and biological features of the primary CLL samples analyzed in this study.

Age, Sex, Rai stage at diagnosis (na: not available), IGHV mutational status (unmutated-CLL, U-CLL; mutated-CLL, M-CLL), Cytogenetics (del: deletion; tri: trisomy; nd: not determined), *SF3B1* mutational status (MUT, mutant; WT, wild type), purity of CLL preparation defined by % CD19⁺CD5⁺ of the total PBMC, as analyzed by flow cytometry (nd: not determined), and *in vitro* assays for which samples were utilized (RNA-seq: RNA sequencing; BH3, BH3 profiling; WB, Western Blot). IGHV gene mutational analysis was performed by PCR, followed by direct sequencing, and 98% cut-off was utilized for mutational status assessment. Percentage homology to germline IGHV sequence is indicated in parenthesis. Cytogenetic abnormalities were determined by fluorescent *in situ* hybridization (FISH), while *SF3B1* mutational status was determined by direct targeted sequencing.

Pt #	Age	Sex	Rai Stage	IGHV status (% homology)	FISH	<i>SF3B1</i> status	Tumor Purity (%)	Assay
1	54	M	0	U-CLL (99.6)	tri12	WT	99.4	RNA-seq, viability, WB
2	50	M	III	U-CLL (100)	Normal	MUT (K700E)	99.6	Viability, BH3
3	65	M	I	U-CLL (100)	del13q, del17p	MUT (K700E)	99.2	RNA-seq, viability, WB
4	45	F	0	M-CLL (97.9)	Normal	WT	99.8	RNA-seq, RT-PCR, viability, BH3
5	64	M	0	U-CLL (99.7)	del17p	WT	99.9	RNA-seq
6	59	F	0	M-CLL (95.8)	del13q, tri12	WT	98.5	RNA-seq, RT-PCR, viability, BH3
7	55	M	I	U-CLL (100)	del11q, del13q	WT	91.9	RNA-seq, RT-PCR, viability, BH3, WB
8	53	F	I	U-CLL (100)	del13q, del 17p	MUT (Q659R)	99.6	RNA-seq, viability, BH3
9	33	F	0	U-CLL (100)	del13q	MUT (T663I)	98.2	RNA-seq, viability, BH3
10	57	F	0	M-CLL (89.1)	del13q	WT	100	RNA-seq, viability, BH3
11	37	M	0	U-CLL (99.7)	del11q, del13q	MUT (G742D)	93.4	RNA-seq, viability
12	58	F	I	U-CLL (100)	del13q	MUT (K666E)	88	RNA-seq, viability, BH3
13	52	F	0	M-CLL (97.2)	nd	WT	99.8	Viability
14	72	M	0	U-CLL (100)	nd	WT	99.5	Viability
15	88	F	II	U-CLL (100)	tri12	MUT(K666 N)	99.4	Viability, BH3
16	53	F	0	U-CLL (100)	del11q, del13q, del17p	MUT (E622D)	98.1	Viability

17	55	M	III	U-CLL (unknown)	del11q, del13q	MUT (K700E)	88.6	Viability, BH3, WB
18	57	F	IV	M-CLL (96)	del11q, del13q	WT	96.1	Viability, BH3, WB
19	66	F	IV	U-CLL (100)	del13q	WT	90.8	Viability, BH3
20	70	F	III	U-CLL (100)	del17p	WT	86.9	Viability, BH3
21	75	F	0	U-CLL (100)	Normal	MUT (G742D)	87.7	Viability, BH3, WB
22	73	M	IV	M-CLL (96)	del11q	MUT (K700E)	nd	Viability, WB
23	46	F	0	U-CLL (unknown)	del13q	MUT (R630I, D894G)	nd	Viability, WB
24	60	M	II	M-CLL (93.7)	tri12	WT	nd	Viability
25	64	M	0	nd	del17p, del13q	WT	nd	Viability
26	64	M	I	U-CLL (100)	del13q	WT	nd	Viability, WB
27	67	M	III	U-CLL (100)	tri12	WT	nd	Viability, WB
28	52	F	I	M-CLL (94.6)	del17p, del13q	WT	nd	Viability, WB
29	53	M	0	U-CLL (100)	Normal	WT	99.8	Viability
30	62	M	0	M-CLL (89.6)	del13q	WT	98.5	Viability
31	71	M	0	U-CLL (99)	del13q	WT	100	Viability
32	42	F	I	M-CLL (92.8)	nd	WT	nd	Viability
33	49	M	na	M-CLL (93)	del17p	MUT (K700E)	nd	Viability
34	58	M	II	U-CLL (99.7)	del11q, del13q	MUT (K666E)	99.9	Viability

Supplemental Table 4, related to Figure 2C and Suppl. Figure 2C.

Pathway enrichment analysis of the 1000 most significant intron retention (IR) and the 1000 most significant cassette exon (CE) events after E7107 treatment, the events with $|\Delta\text{PSI}|>90$, and the events with $|\Delta\text{PSI}|=100$. Pathways enriched within each category, *P* values, and genes within each category are included in the table. “*” highlights the pathways displayed in **Figure 2C** and **Supplemental Figure 2C**.

Top1000 IR	P-value	Genes
*B cell activation_Homo sapiens_P00010	1.890E-05	NFKB1A;CD79B;CD19;BTK;PIK3CD;MAPK1;PTPN6;HRAS;MAPK12;NFKB2
PDGF signaling pathway_Homo sapiens_P00047	2.550E-05	ARHGAP9;GSK3A;STAT2;SRF;PIK3CD;ARHGAP4;RAB11B;AKT2;MKNK2;RPS6KB2;ERF;MAPK1;STAT6;HRAS
*Apoptosis signaling pathway_Homo sapiens_P00006	4.010E-05	MAP4K2;DAXX;ATF6B;TNFRSF10B;PIK3CD;RELA;NFKB2;NFKB1A;AKT2;BAX;AKT1;MAPK1;MCL1
*Ras Pathway_Homo sapiens_P04393	0.0022	GSK3A;SRF;AKT1;PIK3CD;MAPK1;RGL2;HRAS;MAPK12
T cell activation_Homo sapiens_P00053	0.0032	NFKB1A;AKT2;WAS;AKT1;PIK3CD;MAPK1;HRAS;NFKB2
Insulin/IGF pathway-protein kinase B signaling cascade_Homo sapiens_P00033	0.0054	GSK3A;AKT2;INPPL1;PIK3CD;AKT1
Parkinson disease_Homo sapiens_P00049	0.0061	BLK;PSMA4;CSNK1A1;ADRBK1;MAPK1;CSNK1D;UBE2J2;MAPK12
*Interleukin signaling pathway_Homo sapiens_P00036	0.0086	IL4R;AKT2;STAT2;SRF;MKNK2;AKT1;MAPK1;STAT6
Huntington disease_Homo sapiens_P00029	0.0095	DCTN1;AKT2;ARPC1B;BAX;AKT1;AP2A1;DYNLL1;IFT57;ACTG1;ARF6
*p53 pathway_Homo sapiens_P00059	0.0101	HDAC1;AKT2;BAX;AKT1;TNFRSF10B;PIK3CD;MTA2
EGF receptor signaling pathway_Homo sapiens_P00018	0.0117	AKT2;STAT2;PPP2R5B;AKT1;PIK3CD;MAPK1;STAT6;HRAS;MAPK12
*Inflammation mediated by chemokine and cytokine signaling pathway_Homo sapiens_P00031	0.0118	ARPC1B;INPPL1;PIK3CD;RELA;NFKB2;ACTG1;ARPC2;AKT2;GRK6;AKT1;MAPK1;CCR7;ITGB7
*PI3 kinase pathway_Homo sapiens_P00048	0.0132	GNB2;AKT2;RPS6KB2;INPPL1;AKT1
p53 pathway feedback loops 2_Homo sapiens_P04398	0.0175	AKT2;PIK3CD;AKT1;HRAS;MAPK12
FGF signaling pathway_Homo sapiens_P00021	0.0191	AKT2;PPP2R5B;AKT1;PIK3CD;MAPK1;PTPN6;HRAS;MAPK12
*p38 MAPK pathway_Homo sapiens_P05918	0.0221	SRF;MKNK2;MEF2D;MAPK12
*Toll receptor signaling pathway_Homo sapiens_P00054	0.0245	NFKB1A;IRF3;UBE2N;RELA;NFKB2
CCKR signaling map ST_Homo sapiens_P06959	0.0250	NFKB1A;CSNK1A1;SRF;BAX;AKT1;MAPK1;CSNK1D;MEF2D;ARHGAP4;MCL1;HDAC7
Angiotensin II-stimulated signaling through G proteins and beta-arrestin_Homo sapiens_P05911	0.0270	GNB2;ADRBK1;GRK6;MAPK1

p53 pathway by glucose deprivation_Homo sapiens_P04397	0.0326	AKT2;RPS6KB2;AKT1
Salvage pyrimidine ribonucleotides_Homo sapiens_P02775	0.0430	UCK1;NME3
*Hypoxia response via HIF activation_Homo sapiens_P00030	0.0461	AKT2;PIK3CD;AKT1

Top1000 CE	P-value	Genes
PDGF signaling pathway_Homo sapiens_P00047	2.810E-05	ARHGAP9;STAT5A;GSK3A;STAT2;PIK3R2;ELF2;RASA1;MKNK1;RPS6KB2;NCK2;MAPK1;STAT6;PLCG1;RAF1;HRAS
*Cell cycle_Homo sapiens_P00013	0.0003	CCND3;PSMD11;PSMD14;PSMD4;PSMD3
*Ras Pathway_Homo sapiens_P04393	0.0173	GSK3A;MAPK1;RAF1;RGL2;HRAS;RHOA;MAPK12
*Interleukin signaling pathway_Homo sapiens_P00036	0.0184	STAT5A;IL4R;RASA1;MKNK1;STAT2;MAPK1;STAT6;RAF1
Nicotine pharmacodynamics pathway_Homo sapiens_P06587	0.0220	EPB41;GNB1;FLNA;PPP1CA
*B cell activation_Homo sapiens_P00010	0.0227	CD79B;CD19;MAPK1;RAF1;HRAS;MAPK12
T cell activation_Homo sapiens_P00053	0.0229	NCK2;MAPK1;PIK3R2;PLCG1;RAF1;HRAS;NFKB1
Insulin/IGF pathway-mitogen activated protein kinase kinase/MAP kinase cascade_Homo sapiens_P00032	0.0247	RASA1;RPS6KB2;MAPK1;RAF1
EGF receptor signaling pathway_Homo sapiens_P00018	0.0259	STAT5A;RASA1;STAT2;MAPK1;STAT6;PLCG1;RAF1;HRAS;MAPK12
Pyruvate metabolism_Homo sapiens_P02772	0.0360	CS;PKM
Parkinson disease_Homo sapiens_P00049	0.0377	HSPA9;ADRBK1;STX7;CUL1;MAPK1;CSNK1D;MAPK12
Angiotensin II-stimulated signaling through G proteins and beta-arrestin_Homo sapiens_P05911	0.0415	ADRBK1;GNB1;MAPK1;RAF1
TCA cycle_Homo sapiens_P00051	0.0452	CS;SDHC

\DeltaPSI >90	P-value	Genes
PDGF signaling pathway_Homo sapiens_P00047	1.339E-06	ARHGAP9;CHUK;STAT1;STAT2;ARAF;ITPR1;PIK3R2;PIK3CB;FLI1;ARHGAP12;RPS6KA3;MAPK7;PIK3CA;RPS6KB1;RASA1;RASA2;RPS6KA1;PLCG2;PKN2;JAK2
*Ubiquitin proteasome pathway_Homo sapiens_P00060	5.885E-05	SMURF2;UBE3C;PSMD4;PSMD13;UBA6;UBA3;UBA2;UBE2D1;WWP2;UBE2K
T cell activation_Homo sapiens_P00053	0.0004	PPP3CB;PPP3CC;HLA-DMB;PIK3CA;CHUK;ARAF;ITPR1;WAS;LCP2;PIK3R2;PIK3CB;NFKB1

EGF receptor signaling pathway_Homo sapiens_P00018	0.0017	STAT1;STAT2;PPP2R5B;PPP2R5D;PPP2R5C;PIK3CB;MAPK13;PIK3CA;RRAS;RASA1;RASA2;PLCG2;MAP3K4;MAP3K5
FGF signaling pathway_Homo sapiens_P00021	0.0020	PPP2R5B;PPP2R5D;PPP2R2A;PPP2R5C;PIK3CB;MAPK13;PIK3CA;PPP2R1B;RASA1;RASA2;PLCG2;MAP3K4;MAP3K5
*Apoptosis signaling pathway_Homo sapiens_P00006	0.0026	ATF2;CHUK;PIK3CB;IGF2R;NFKB1;BCL2L11;CASP8;PIK3CA;MADD;REL;FAS;RIPK1;MAP3K5
*Interleukin signaling pathway_Homo sapiens_P00036	0.0052	RPS6KA3;IL4R;MAPK7;PIK3CA;CHUK;STAT1;RASA1;STAT2;RPS6KA1;ARAF;PIK3CB
*Hypoxia response via HIF activation_Homo sapiens_P00030	0.0072	EGLN1;CREBBP;PIK3CA;PIK3R2;PIK3CB
*Cell cycle_Homo sapiens_P00013	0.0082	PSMD4;PSMD13;PSMD3;ANAPC10
*B cell activation_Homo sapiens_P00010	0.0093	PPP3CB;PIK3CA;CHUK;ARAF;ITPR1;PLCG2;PIK3CB;MAPK13
*Ras Pathway_Homo sapiens_P04393	0.0097	ATF2;RPS6KA3;PIK3CA;STAT1;RPS6KA1;ARAF;PIK3CB;MAP3K4;MAPK13
*Notch signaling pathway_Homo sapiens_P00045	0.0134	APH1A;NEURL4;NCSTN;MFNG;NUMB;RBPJ
Insulin/IGF pathway-mitogen activated protein kinase kinase/MAP kinase cascade_Homo sapiens_P00032	0.0163	RPS6KA3;RPS6KB1;RASA1;RPS6KA1;IGF2R
Axon guidance mediated by netrin_Homo sapiens_P00009	0.0187	VASP;PIK3CA;PLCG2;PIK3R2;PIK3CB
Mannose metabolism_Homo sapiens_P02752	0.0357	GMPPB;PMM2
Coenzyme A biosynthesis_Homo sapiens_P02736	0.0357	PANK4;PANK2

 \DeltaPSI =100	P-value	Genes
*B cell activation_Homo sapiens_P00010	0.0021	PPP3CB;CHUK;ARAF;ITPR1;PLCG2
*Apoptosis signaling pathway_Homo sapiens_P00006	0.0059	ATF2;BCL2L11;CHUK;FAS;IGF2R;MAP3K5
*Ubiquitin proteasome pathway_Homo sapiens_P00060	0.0048	SMURF2;UBE3C;UBA6;UBA2
T cell activation_Homo sapiens_P00053	0.0062	PPP3CB;CHUK;ARAF;ITPR1;PIK3R2
PDGF signaling pathway_Homo sapiens_P00047	0.0092	CHUK;RASA2;ARAF;PLCG2;ITPR1;PIK3R2

REFERENCES

1. Wang L, Brooks AN, Fan J, et al. Transcriptomic Characterization of SF3B1 Mutation Reveals Its Pleiotropic Effects in Chronic Lymphocytic Leukemia. *Cancer Cell*. 2016;30(5):750-763.